The seismic equation of state used by *Ahrens et al.* [1969] to constrain the zero-pressure properties of the high-pressure phases was

$$\rho_0 = 0.048\langle M\rangle\Phi_0^{0.323} \quad (5)$$

This resulted from fitting the zero-pressure properties of a selection of 31 rocks and minerals, which included many with open crystal structures such as α-quartz and feldspars [*D. L. Anderson*, 1967]. It was pointed out by *D. L. Anderson* [1969] that the equation

$$\rho_0 = 0.0492\langle M\rangle\Phi_0^{1/3} \quad (6)$$

gave a good fit to the zero-pressure properties of MgO, Al_2O_3, and SiO_2 (stishovite), all of which have close-packed crystal structures. Equation 6 thus seems more appropriate to describe the zero-pressure properties of the close-packed phases to be expected in the lower mantle. The results presented here support this conjecture.

Comparison of Results using Old and New Seismic Equations of State

The results of the analysis of the shock-wave data when the original (equation 5) and revised (equation 6) equations of state are used are given in Table 1 and Figures 1 and 2. Table 1 lists the Birch-Murnaghan parameters ρ, K_0, and ξ of the 'ambient' adiabat (i.e., centered at 300°K and $P = 0$) of each material considered. Also listed are K_0', from (2), and Φ_0, the zero-pressure value of the seismic parameter $\Phi_0 = (\partial P/\partial\rho)_S = K_S/\rho$, where the subscript S indicates constant entropy.

The difference between the original and re-

TABLE 1. Parameters of the Ambient Adiabats Derived Using the Original and Revised Seismic Equations of State

	$\rho_0 = 0.048\langle M\rangle\Phi^{0.323}$					$\rho_0 = 0.0492\langle M\rangle\Phi^{1/3}$				
	ρ_0, g/cm³	K_0, Mb	ξ	K_0'	Φ_0, (km/sec)²	ρ_0, g/cm³	K_0, (Mb)	ξ	K_0'	Φ_0, (km/sec)²
Forsterite (Fo)	4.31	4.425	2.22	1.05	103	4.18	3.186	0.88	2.83	76
Olivinite I (Oliv)	4.58	4.840	0.86	2.85	106	4.28	2.961	0.48	3.35	69
Twin Sisters dunite (TS)	4.12	3.367	1.01	2.65	82	3.94	2.147	0.41	3.45	55
Hortonolite dunite (Ho)	4.75	3.319	1.22	2.37	70	4.59	2.366	0.65	3.14	52
Fayalite (Fa)	5.31	3.319	1.87	1.50	63	5.03	2.173	0.89	2.81	43
Hematite (Fe_2O_3)	5.96	3.991	1.52	1.98	67	5.70	2.727	0.83	2.89	48
Magnetite (Fe_3O_4)	6.30	4.488	1.66	1.79	71	6.11	3.225	0.94	2.74	53
Spinel (Sp)	4.19	3.819	1.06	2.59	91	4.03	2.646	0.53	3.29	65
Enstatite (Ens)	4.20	4.031	4.23	−1.64	96	3.93[c]	...	...	...	...
Bronzitite (Br)	3.74	2.117	1.14	2.48	57	3.33	1.086	0.49	3.34	33
Sillimanite (Sill)	4.00	3.187	1.40	2.33	80	3.94	2.435	0.82	2.91	62
Andalusite (And)	3.95	3.045	1.16	2.46	77	3.84	2.185	0.61	3.19	57
Anorthosite (An)	3.71	2.084	1.20	2.40	56	3.57	1.481	0.67	3.11	41
Oligoclase (Olig)	3.69	2.198	1.60	1.87	60	3.57	1.592	0.72	3.15	45
Albitite (Alb)	3.81	2.550	1.63	1.82	67	3.69	1.84	0.71	3.05	50
Microcline (Micr)	3.50	1.563	1.47	2.04	45	3.36	1.09	0.70	3.06	33
Westerly granite (WGr)	3.96	2.907	1.32	2.24	73	3.90	2.22	0.75	3.00	57
Eclogite (Ecl)	3.61	1.555	0.76	2.99	43	3.49	1.12	0.39	3.48	32
Periclase (MgO)	3.584[a]	1.628	0.11	3.85	45					
Corundum (Al_2O_3)	3.988[a]	2.551	−0.12	4.16	64					
Stishovite (SiO_2)	4.287[a]	3.546	0.66	3.12	83					
Wustite (FeO)	5.86[a,b]	...	...	...	30[b]					
	$\rho_0 = 0.051\langle M\rangle\Phi^{1/3}$									
Fayalite	4.82	1.65	0.67	3.10	34					
Hematite	5.44	2.03	0.58	3.23	37					
Magnetite	6.00	2.69	0.72	3.05	45					

[a] Fixed density.
[b] Extrapolated from $Fe_{.98}O$ [*Clark*, 1966; *D. L. Anderson*, 1969].
[c] From hugoniot.

vised results is most strikingly illustrated by Figures 1 and 2. In these figures, the loci of the ambient adiabats have been plotted in the log $(\rho/\langle M\rangle)$ — log Φ plane (note that $\langle M\rangle/\rho$ is the molar volume). In this plane the seismic equations of state (5) and (6) are straight lines (of slopes 0.323 and 1/3, respectively). The zero-pressure ends of the adiabatic curves all fall on the seismic equation of state line, with pressure increasing away from the line along each adiabat. It can be seen that the original adiabats in Figure 1 are much less orderly than the revised adiabats in Figure 2, and that for many of the original adiabats Φ becomes a decreasing function of ρ (and P) at higher pressures, whereas this does not occur in Figure 2.

From the definitions $K = \rho\, dP/d\rho$ and $\Phi = K/\rho$, it can readily be shown that for any given function $P = P(\rho)$.

$$\frac{d(\log \Phi)}{d(\log \rho)} = \frac{dK}{dP} - 1 \qquad (7)$$

Thus a slope of 1/3 in the log $(\rho/\langle M\rangle)$ — log Φ plane corresponds to $dK/dP = 4$, and a slope of -1 corresponds to $dK/dP = 0$. The theoretical high-pressure limit on dK/dP, as given by the Thomas-Fermi approximation, is 5/3 [*March*, 1955], which corresponds to a slope of 3/2 in Figures 1 and 2. (Lines of slope 1/3, 3/2, and -1 are shown in Figure 1 for comparison.) Clearly, for many of the original adiabats (Figure 1) dK/dP falls below the Thomas-Fermi limit at high pressures, and for some it falls below zero. For the revised adiabats (Figure 2), dK/dP approaches the Thomas-Fermi limit at high pressures in some cases, but usually is substantially greater.

The revision has had the additional effect that at all pressures the range of values of dK/dP for the substances considered is much narrower. This narrow range is illustrated by the range of slopes of the adiabats in Figure 1 as compared to Figure 2, and also, at zero pressure, by the values of K_0' given in Table 1. The original

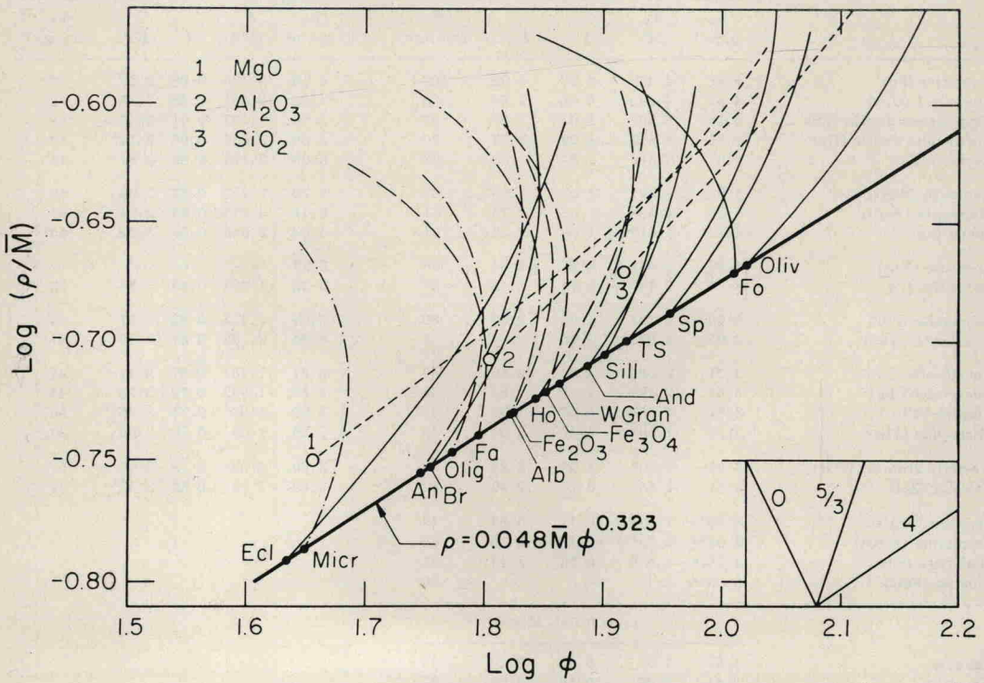

Fig. 1. Log $(\rho/\langle M\rangle)$ — log Φ plot of adiabats derived using equation 5. Straight line is seismic equation of state line, equation 5. Short-dashed curves, oxides; long-dashed curves, iron-rich compounds; dash-dot curves, rocks containing feldspars; solid curves, others listed in Tables 1 and 2. Abbreviations are identified in Table 1. Inset: lines with slopes corresponding to $dK/dP = 0$, 5/3, and 4, as labeled.